A peer-reviewed version of this preprint was published in PeerJ on 12 June 2018.

View the peer-reviewed version (peerj.com/articles/4956), which is the preferred citable publication unless you specifically need to cite this preprint.

Choi JI, Lee HK, Kim HS, Park SY, Lee TY, Yoon K, Lee JI. 2018. Odor-dependent temporal dynamics in *Caenorhabitis elegans* adaptation and aversive learning behavior. PeerJ 6:e4956
https://doi.org/10.7717/peerj.4956

PeerJ Preprints NOT PEER-REVIEWED

Odor-dependent temporal dynamics in *C. elegans* odor memory

Jae Im Choi [1], **Hee Kyung Lee** [1], **Hae Su Kim** [1], **So Young Park** [1], **Kyoung-hye Yoon** [Corresp., 1], **Jin I Lee** [Corresp. 1]

[1] Division Of Biological Science and Technology, Yonsei University, Wonju, Gangwondo, South Korea

Corresponding Authors: Kyoung-hye Yoon, Jin I Lee
Email address: kyounghyeyoon@yonsei.ac.kr, jinillee@yonsei.ac.kr

Animals sense an enormous number of cues in their environments, and, over time, can form memories and associations to some of these. The nervous system remarkably maintains the specificity of memory to each of the cues. Here we asked whether the nematode *Caenorhabditis elegans* adjusts the temporal dynamics of odor memory formation depending on the specific odor sensed. *C. elegans* senses a multitude of odors, and memory formation to some of these odors requires activity of the cGMP-dependent protein kinase EGL-4 in the AWC sensory neuron. We identified a panel of 17 attractive odors, some of which have not been tested before, and determined that the majority of these odors require the AWC primary sensory neuron for sensation. We then devised a novel assay to assess odor behavior over time for a single population of animals. We used this assay to evaluate the temporal dynamics of memory formation to 13 odors and find that memory formation occurs early in some odors and later in others. We then examined EGL-4 localization in early-trending and late-trending odors over time and found that the timing of memory formation correlated with the timing of nuclear accumulation of EGL-4 in the AWC neuron. We demonstrate that odor memory formation in *C. elegans* can be used as a model to study the timing of memory formation to different sensory cues.

PeerJ Preprints NOT PEER-REVIEWED

1 **Title: Odor-dependent temporal dynamics in *Caenorhabitis elegans* odor memory**

2 **Authors:** Jae Im Choi**, Hee Kyung Lee**, Hae Su Kim**, So Young Park**, Kyoung-hye Yoon*,

3 Jin I. Lee*

4

5

6 **Affiliation:** Division of Biological Science and Technology

7 Yonsei University

8 1 Yonseidae-gil

9 Wonju, Gangwondo

10 South Korea 26493

11

12 **Correspondence should be addressed to:**

13 Jin I. Lee (jinillee@yonsei.ac.kr)

14 Kyoung-hye Yoon (kyounghyeyoon@yonsei.ac.kr)

15

16

17

18 * Co-corresponding authors

PeerJ Preprints | https://doi.org/10.7287/peerj.preprints.26451v1 | CC BY 4.0 Open Access | rec: 22 Jan 2018, publ: 22 Jan 2018

** Co-first authors

ABSTRACT

Animals sense an enormous number of cues in their environments, and, over time, can form memories and associations to some of these. The nervous system remarkably maintains the specificity of memory to each of the cues. Here we asked whether the nematode *Caenorhabditis elegans* adjusts the temporal dynamics of odor memory formation depending on the specific odor sensed. *C. elegans* senses a multitude of odors, and memory formation to some of these odors requires activity of the cGMP-dependent protein kinase EGL-4 in the AWC sensory neuron. We identified a panel of 17 attractive odors, some of which have not been tested before, and determined that the majority of these odors require the AWC primary sensory neuron for sensation. We then devised a novel assay to assess odor behavior over time for a single population of animals. We used this assay to evaluate the temporal dynamics of memory formation to 13 odors and find that memory formation occurs early in some odors and later in others. We then examined EGL-4 localization in early-trending and late-trending odors over time and found that the timing of memory formation correlated with the timing of nuclear accumulation of EGL-4 in the AWC neuron. We demonstrate that odor memory formation in *C. elegans* can be used as a model to study the timing of memory formation to different sensory cues.

INTRODUCTION

39 The ability to form memories to odors is inherent to most animals. In particular, the
40 formation of memories to biologically pertinent odors can be important for survival and
41 reproduction. For instance, mother sheep form specific odor memories of their own lambs
42 rather than other stranger lambs within hours of birth (Broad et al. 2002). This specific odor
43 memory formation will be important for the mother sheep to establish bonding behaviors with
44 her young (Levy et al. 2004).

45 The formation of a memory involves a step-by-step process defined by molecular and
46 cellular activities within a determined circuitry. After a cue from the environment is recognized,
47 the first stop along the path of the memory trace is a short-term memory (STM). In the sea snail
48 *Aplysia*, short-term or intermediate-term memory in response to touch requires cell signaling
49 events in the sensory neurons themselves (Ghirardi et al. 1995; Hawkins et al. 2006; Klein et al.
50 1982; Montarolo et al. 1986). Upon a strong and persistent cue, a robust and stable long-term
51 memory (LTM) can form in response to changes in gene transcription and protein translation in
52 *Aplysia* (Castellucci et al. 1970; Castellucci et al. 1989; Sutton et al. 2001). These changes
53 require the kinase PKA to translocate from the cytoplasm to the nucleus to phosphorylate
54 nuclear substrates and activate gene expression (Bacskai et al. 1993). The transition to long-
55 term memory can be blocked and enhanced by a number of factors. For instance increased
56 tyrosine kinase activity can reduce the cue threshold for long-term memory and enhance the
57 LTM response, implicating that growth factors may facilitate LTM formation (Purcell et al.
58 2003). In addition, the phosphatase calcineurin can block the induction of LTM by counteracting
59 kinase activity (Mansuy et al. 1998).

60 The nematode *Caenorhabditis elegans* is attracted to dozens or more odors and forms a
61 memory in response to persistent odor stimulation in the absence of food (Bargmann et al.
62 1993; Colbert & Bargmann 1995; Ward 1973). A short 30 minute exposure to the odor
63 benzaldehyde attenuates the attraction transiently. However, an 80 minute exposure
64 eliminates the attraction for benzaldehyde for a prolonged period (Colbert & Bargmann 1995;
65 Lee et al. 2010). Short-term memory to benzaldehyde requires kinase activity in the cytoplasm
66 by the *C. elegans* PKG homolog EGL-4, whereas long-term odor memory requires EGL-4 to
67 translocate to the nucleus and phosphorylate nuclear targets (Juang et al. 2013; L'Etoile et al.
68 2002; Lee et al. 2010; O'Halloran et al. 2009), similar to PKA nuclear translocation in *Aplysia*.

69 Although benzaldehyde odor memory has been thoroughly investigated, it is unknown
70 whether strong memories to certain odors can form faster than to other odors. In this study we
71 sought to investigate the temporal dynamics of memory formation to a large panel of odors by
72 designing a new odor behavior assay called the real-time odor behavior assay. Using this novel
73 assay, we found the timing of memory formation was specific for each odor, and temporal
74 dynamics were correlated to the localization of EGL-4 in the AWC neuron.

75

76 **MATERIALS AND METHODS**

77 *Nematode culture and strains*. Worms were grown and maintained at 20°C on Nematode
78 Growth Medium (NGM) plates seeded with E. coli OP50 as described previously (Brenner 1974).
79 Strains used for this study, N2, *ceh-36*, *odr-7, pyIs500* ((p)*odr-3*::GFP::*egl-4*), were obtained
80 from the *Caenorhabditis* Genetic Center (University of Minnesota, USA).

81

82 *Behavior assays.* Standard odor chemotaxis assays were carried out using previously
83 established protocols with a few changes (Bargmann et al. 1993). The following odors were
84 used: benzaldehyde, butanone, isoamyl alcohol (Sigma-Aldrich, USA); isobutyric acid, 2-isobutyl
85 thiazole, dimethylthiazole, 2,4,5-trimethylthiazole, 2-methylpyrazine, 2-heptanone, 4-
86 chlorobenzyl mercaptan, butyric acid, 1-pentanol, benzyl mercaptan, 2-cycolhexylethanol,
87 benzyl proprionate (Alfa Aesar, South Korea); 1-methylpyrrole, 2-ethoxythiazole (TCI, Japan);
88 diacetyl (Acros Organics, Belgium). All odors were diluted from original stock to a 1:100 dilution
89 with ethanol except for benzaldehyde (1:200) and 2,4,5-trimethylthiazole (1:1000). A total of 4
90 µl of diluted odor or ethanol was placed on the assay plate as attractant and counterattractant,
91 respectively. 2 µl of NaN_3 was placed with the attractant and counterattractant. Briefly, adult
92 worms were washed in S-basal buffer (5.85 g NaCl, 1 g K_2HPO_4, 6 g KH_2PO_4) 3 times, placed on
93 the assay plate, and allowed to move freely for at least one hour before counting.

94 Standard odor memory behavior assays were carried out similar to previous published
95 protocols (Colbert & Bargmann 1995). Before assaying behavior, worms were washed in S-basal
96 buffer 3 times, and placed in 1 ml of benzaldehyde or 2,4,5-TMT diluted at 1:10,000 in S-basal
97 buffer for 0-120 minutes at 10 minute or 20 minute intervals. After odor exposure, worms were
98 washed 3 times in S-basal and behavior was assayed.

99

100 *Real-time odor behavior assay.* Media for the assay plate is as follows: 1.6% Difco Granulated
101 Agar (BD, USA) was dissolved in water by heating, and 1mM of $CaCl_2$, 1mM of $MgSO_4$ and 5 mM

102 of KPO_4 buffer (108.3 g KH2PO4, 35.6 g K2HPO4, H2O to 1 liter) was mixed with the agar. Media
103 was dispensed into 12.5 cm X 12.5 cm X 2 cm square plastic culture plates (SPL Bioscience, S.
104 Korea), and allowed to harden for at least 3 hours. Odors were diluted with ethanol to the
105 following concentrations: benzaldehyde (1:100), butanone (1:100), diacetyl (1:100), isoamyl
106 alcohol (1:1000), 2-heptanone (1:1000), 2,4,5-TMT (1:500), 4-chlorobenzyl mercaptan (1:500),
107 2-ethoxythiazole (1:300), 2-cyclohexylethanol (1:5000), 1-methylpyrrole (1:500), 1-pentanol
108 (1:10000), 2-isobutylthiazole (1:100), 2-methylpyrazine (1:10). Diluted attractant odors were
109 placed in the middle of the "A" section of the assay plate (Figure 1), and a dab of OP50 strain *E.*
110 *coli* bacteria from a standard nematode growth media plate with a platinum worm picker was
111 placed in the middle of the "F" section of the assay plate as a counterattractant, no larger than
112 3 mm diameter. The counterattractant itself is a very weak attractant (Figure 1B, control), and
113 overall aids this assay in resolving the attenuation of odor attraction after memory has formed.
114 Washed worms are then placed in the middle of the plate, and dried by wicking the buffer using
115 an unscented tissue. The plates were tapped somewhat vigorously which aids in worm
116 movement away from the center of the plate. Worms were counted in each section A, B, E, and
117 F every ten minutes for 120 minutes and attraction index was calculated. 50% total behavior
118 change was calculated as (30 min AI – 120 min AI)/2.

119

120 *Quantification of GFP::EGL-4 localization*. Subcellular localization of GFP::EGL-4 in *py*Is500
121 ((p)*odr-3*::GFP::EGL-4; (p)*odr-1*::RFP) integrated strain worms during odor memory formation
122 was performed as previously published (Lee et al. 2010). Briefly, *py*Is500 animals were exposed
123 to odor dilutions of either benzaldehyde (1:10000), 2-ethoxythiazole (1:10000), 1-methylpyrrole

124 (1:10000), 4-chlorobenzyl mercaptan (1:5000), or 2,4,5-TMT (1:10000) in S-basal for 0-120
125 minutes at 20 minute intervals. After odor exposure, worms were placed on slides containing a
126 2% agar dried pad with 1 µl of 1M NaN_3 added to anesthetize the animals and observed under a
127 fluorescent microscope. At least 20 animals were counted per sample, and EGL-4 localization
128 was determined as either cytoplasmic or nuclear in the AWC neuron for each animal. After the
129 data was plotted, a polynomial regression equation was determined (Microsoft Excel) for each
130 odor as follows: benzaldehyde (y = 0.0308x4 - 1.1348x3 + 10.026x2 - 17.514x + 16.786), 2-
131 ethoxythiazole (y = -0.1198x4 + 1.0243x3 - 0.599x2 + 4.9802x + 5.5179), 1-methylpyrrole (y = -
132 0.2053x4 + 2.3015x3 - 5.4917x2 + 4.5729x + 8.4286), 4-chlorobenzyl mercaptan (y = -0.1454x4 +
133 1.8802x3 - 6.4253x2 + 11.766x + 1.0536), 2,4,5-TMT (y = 0.1437x4 - 2.599x3 + 15.825x2 -
134 27.302x + 22.06). Equations were used to calculate the approximate time at which 50% of
135 animals display nuclear EGL-4.

136

137 **RESULTS**

138 **Attraction to novel odors mediated by the AWC or the AWA primary sensory neurons**

139 *C. elegans* is attracted to dozens of odors (Bargmann et al. 1993), and several forms of
140 memory to a few of these odors have been demonstrated (Colbert & Bargmann 1995;
141 Kauffman et al. 2010; L'Etoile et al. 2002; Torayama et al. 2007). To test the olfactory memory
142 to a larger panel of odors, we screened through a large set of over 150 odor chemicals and
143 identified dozens of attractive odors. From this smaller group, we tested attraction to a subset

144 of 18 highly attractive odors in wild-type and olfactory sensory neuron mutants in a standard
145 chemotaxis assay (Bargmann et al. 1993).

146 Odor attraction in *C. elegans* is mediated by two pairs of olfactory sensory neurons, the
147 AWC neurons and the AWA neurons. Mutants of the *ceh-36* gene which encodes an *Otx*
148 homeodomain transcription factor do not develop AWC olfactory sensory neurons (Lanjuin et
149 al. 2003), whereas mutants of the *odr-7* gene which encodes an AWA-specific nuclear hormone
150 receptor lack the AWA sensory neurons (Sengupta et al. 1994). Thus, AWC-sensed odors such as
151 benzaldehyde or butanone are unable to be sensed in *ceh-36* mutants, and, conversely, AWA-
152 sensed odors such as diacetyl are no longer sensed in *odr-7* mutants. As predicted, we show
153 that diacetyl attraction is lost in the AWA- *odr-7* mutants and maintained in *ceh-36* mutants
154 (Table 1). On the contrary, benzaldehyde attraction disappears in the AWC- *ceh-36* mutants but
155 is normal in AWA- *odr-7* mutants. Finally, 2,4,5-trimethylthiazole which is sensed by both AWA
156 and AWC neurons remains attractive in both AWC- and AWA- mutants. When we tested the
157 other odors, we found that attraction to most of the odors required the AWC sensory neurons,
158 with only butyric acid and isobutyric acid sensed by the AWA neuron (Table 1). Benzyl
159 proprionate attraction was effectively lost in both AWC- and AWA- mutants. Hence, we have
160 identified many novel attractive AWC-sensed odors.

161

162 **A novel assay to track real-time odor behavior**

163 Short-term and long-term olfactory memory has been studied for the AWC-sensed odor
164 benzaldehyde (Colbert & Bargmann 1995; L'Etoile et al. 2002; Lee et al. 2010). However, the

temporal dynamics of memory formation to other odors have not been tested thoroughly. Thus, we sought to characterize the change in odor attraction over time to a multitude of AWC-sensed odors. The standard odor treatment and chemotaxis assay protocol to measure *C. elegans* odor memory is a robust assay that has led to the discovery of odor memory mutants and revealed molecular pathways involved in memory formation (Bargmann et al. 1993; Colbert & Bargmann 1995; L'Etoile et al. 2002; Lin et al. 2010; O'Halloran et al. 2009). However, for a thorough temporal characterization of memory behavior for multiple odors, the standard assay would require a separate behavior assay for each time point for each odor, necessitating an inordinately large amount of worms and resources for such a study.

Due to the limitations of the standard odor memory behavior assay, we designed a new odor behavior assay we call the "real-time odor behavior assay". This method is based on a previously designed odor behavior assay (Remy & Hobert 2005), in which a population of worms is placed on the center of a larger 12.5 cm X 12.5 cm square plate rather than the 9 cm diameter circular plate used in the standard assay (Fig 1A). The plate is divided into 6 even columns labeled A-F, with a dilution of odor placed in the center of one of the side columns (column A). On the opposite side column (column F), a small spot of OP50 strain *E. coli* bacteria, a common laboratory source of food for *C. elegans*, is placed towards the middle and used as a counterattactant to the odor.

Worms can freely move throughout the whole plate for the entire 120 minute assay. We calculate the "attraction index" to the odor as AI = [[2(# of worms in A) + (# of worms in B)] – [(# of worms in E) + 2 (# of worms in F)]] / 2(# of worms in A+B+E+F), and the attraction index is counted every 10 minutes. Animals in the middle columns C and D where the worms originated

187 from are not counted. Thus, the maximum AI is 1.0 and the minimum AI is -1.0. In contrast to
188 the control assay in which only the diluent ethanol without odor is placed in column A, worms
189 exposed to a dilution of benzaldehyde in the real-time assay move towards the odor for the
190 first 30 minutes, with many animals reaching the attractive odor by 40 minutes (Figure 1B).
191 After another 30 minutes we observed a slight decline in attraction, and finally at 90 minutes
192 we observed a steep decline in attraction that maintained until the end of the assay.

193

194 **Short-term and long-term memory in the real-time odor behavior assay**

195 In the standard behavior assay, continuous odor exposure in the absence of food for
196 about 30 minutes results in a partial and transient attenuation of attraction to benzaldehyde
197 ((Colbert & Bargmann 1995; L'Etoile et al. 2002); Figure 2A). This short-term memory requires
198 activity of the cGMP-dependent protein kinase EGL-4 (L'Etoile et al. 2002) and the cyclic
199 nucleotide-gated channel subunit CNG-3 (O'Halloran et al. 2017). *cng-3* mutants do not display
200 short-term odor memory, but display normal long-term memory to benzaldehyde ((O'Halloran
201 et al. 2017); Fig 2A), which occurs after over 80 minutes of continuous benzaldehyde exposure.
202 On the other hand, the dominant mutation *adp-1* displays no odor memory even after a 120
203 minute odor exposure ((Colbert & Bargmann 1995); Fig 2A).

204 In contrast to the standard assay technique in which odor exposure precedes the
205 behavior assay, animals are concurrently exposed to benzaldehyde as the real-time assay
206 proceeds. In the beginning of the assay, most of the freely moving worms can reach the odor at
207 the far end of the plate within 30 minutes. Thus, to compare the two assay techniques, we

208 consider the 30 minute time point to be the "beginning" of the memory assay similar to the 0
209 minute time point in the standard assay. After the 30 minute time point wild-type *C. elegans*
210 begins to display a decreased attraction for the next 40 minutes similar to that observed during
211 short-term memory in the standard assay (Fig 2A, 2B). In *cng-3* mutants, however, this early
212 change in behavior appears to be absent (Fig 2A, 2B).

213 A major difference between the two assay techniques is that each time point in the
214 standard assay is an independent population of animals, whereas a single population is being
215 tracked in the real-time assay. Thus, each data point is dependent on the previous data point in
216 the real-time assay. This can lead to a decrease in resolution in data over time especially at
217 close time points. To confirm that the real-time assay can indeed measure odor memory states
218 in *C. elegans* similar to the standard assay, we compared attraction at the 0 and 40 minute time
219 points in the standard assay to the 30 and 70 minute time points in the real-time assay. In both
220 the standard and real-time assays, wild-type N2 animals display a significant decrease in
221 attraction after 40 minutes (Fig 2C). Interestingly, this decrease was absent in short-term
222 memory-defective *cng-3* mutants for both the standard and real-time assays (Fig 2C). However,
223 a significant drop in attraction was observed after 80 minutes in both N2 and *cng-3* mutants,
224 showing that long-term memory is intact in *cng-3* mutants (Fig 2B). Finally, no memory to
225 benzaldehyde develops in *adp-1* mutants in either the standard assay or the new assay (Fig 2A,
226 2B). Thus, both short-term and long-term memory can be resolved in the real-time behavior
227 assay.

228

229 **Timing of odor memory formation varies by odor**

230 Since we demonstrated that our assay can accurately assess the timing of benzaldehyde
231 memory, we conducted a comprehensive temporal analysis of memory to a palette of 12 other
232 odors, 9 of which have never been tested for memory. These include alcohols, ketones, thiols,
233 thiazoles, aromatics, and pyrazines. 30 minutes into the assay when we start the analysis, we
234 observe differences in attraction to each odor ranging from 0.91 AI (2,4,5-trimethylthiazole) to
235 0.50 AI (2-heptanone). However, over time, the total decrease in attraction to all of the odors is
236 similar over the entire assay (average AI decrease=-0.475±0.025) with one exception, the odor
237 cyclohexylethanol, which displays only a modest attenuation (AI decrease=-0.19).

238 Among the panel of 13 odors tested, 12 of these odors are sensed by the AWC neuron.
239 One can observe a distinct pattern of change in worm behavior towards these twelve odors
240 over time. For AWC-sensed odors, behavior change generally occurs relatively slowly at the
241 beginning of the assay then proceeds more quickly towards the end (Figure 3). The exception to
242 this is the odor diacetyl, which is the only odor here not sensed by the AWC neuron. Behavior
243 change towards diacetyl appears to arise early and fairly consistently during the entire assay
244 (Figure 3).

245 Although overall memory formation patterns over the 120 minute assay is similar for
246 most of the odors tested, the timing of memory formation varies depending on the odor. For
247 instance, benzaldehyde attraction decreases overall from 0.79 AI to 0.27 from 30 to 120
248 minutes, and 50% of this behavior change occurs within the 90 minute mark (Figure 3; Table 2).
249 This early trend was similar to that of 2-ethoxythiazole attraction (90 min) and 1-methylpyrrole

250 attraction (80 minutes). On the other hand, late trends of behavior change were observed in
251 2,4,5-trimethylthiazole (2,4,5-TMT) attraction (100 minutes) and 4-chlorobenzyl mercaptan (4-
252 CB) attraction (110 minutes) (Figure 3, Table 2). To confirm whether the late change in behavior
253 was actually a result of odor memory, we tested the attraction of *adp-1* mutants to 4-
254 chlorobenzyl mercaptan and 2,4,5-TMT attraction in the real-time assay (Figure S1). Wild-type
255 animals showed large decreases in attraction over the whole assay for both 4-CB (change in
256 AI=-0.478) and 2,4,5-TMT (change in AI=-0.349). However, the change in behavior over time
257 was minimal in *adp-1* mutants for both 4-CB attraction (change in AI=-0.226) and 2,4,5-TMT
258 attraction (change in AI=-0.009). Thus, the late trend in decreased odor attraction for the two
259 odors is likely due to late odor memory formation. We also confirmed that the early trend in
260 benzaldehyde memory and the late trend in 2,4,5-TMT memory can be observed using either
261 the real-time assay or the standard assay (Figure S2). Thus, temporal dynamics of memory
262 formation varies depending on the specific odor.

263

264 **Timing of odor memory formation correlates with the timing of EGL-4 nuclear localization**

265 With the exception of diacetyl which is sensed only by the AWA neuron, all the odors we
266 tested in the real-time assay are sensed by the AWC neuron (Table 1). Odor memory to AWC-
267 sensed odors requires EGL-4 activity: cytoplasmic EGL-4 activity directs short-term memory
268 whereas long-term memory requires EGL-4 to translocate to the nucleus and phosphorylate
269 nuclear targets (Juang et al. 2013; L'Etoile et al. 2002). We wondered whether the changes in
270 odor attraction we observe over time in the real-time assay were correlated to the sub-cellular

271 localization of a functional GFP-tagged EGL-4 in the AWC neuron. We exposed worms to the
272 early-trending odors (benzaldehyde, 2-ethoxythiazole, 1-methylpyrrole) and the late-trending
273 odors (2,4,5-trimethylthiazole, 4-chlorobenzyl mercaptan) and observed EGL-4 localization in
274 the AWC neuron every 20 minutes for 2 hours. Whereas the odor butanone is sensed by one of
275 the AWC neuron pair and EGL-4 nuclear translocation is induced in only one of the AWC
276 neurons, all the odors tested here could induce EGL-4 translocation in both AWC neurons
277 indicating that these odors are likely sensed by both AWC neurons. The maximal percent of
278 animals with nuclear EGL-4 ranged from 60% to almost 80% for each odor (Figure 4). However,
279 neither longer odor incubation nor varying odor concentration could increase maximal nuclear
280 EGL-4 for benzaldehyde, 4-chlorobenzyl mercaptan or 2,4,5-trimethylthiazole (data not shown).

281 The temporal dynamic of EGL-4 nuclear localization in response to the early- and late-
282 trending odors seems to vary depending on the odor. To analyze this in detail, we calculated a
283 polynomial regression for the time curves for each odor (Figure 4), and then estimated the time
284 at which 50% EGL-4 nuclear localization was reached for each odor (Table 2). We found that
285 EGL-4 nuclear localization occurred much faster in the early trending odors (59.2 min, 69.7 min,
286 76.6 min for 2-ethoxythiazole, benzaldhehyde and 2-methylpyrrole, respectively), and occurred
287 much later in the late-trending odors (88.4 min and 90.96 min for 4-CB and 2,4,5-TMT,
288 respectively). Thus, we saw a correlation between the timing of EGL-4 nuclear translocation and
289 the timing of odor memory formation. Taken together, we believe that the timing of odor
290 memory formation for AWC-sensed odors may be regulated by EGL-4 sub-cellular localization.

291

292 **DISCUSSION**

293 Establishing the real-time behavior assay was the key to comprehensively testing
294 temporal dynamics of memory to multiple odors. This assay has several advantages to the
295 standard assay that has been valuable in understanding odor behavior in *C. elegans*. Firstly,
296 tracking a single population over time rather than independent populations at each time point
297 has benefits. For instance, we can observe actual changes in the behavior of animals over time,
298 decrease experimental variability between populations, and save time and resources tracking
299 one population rather than 13 populations over the 120 minute assay. Finally, the real-time
300 assay is a better simulation of odor behaviors in natural habitats than the standard assay. Our
301 group previously showed that production of the odor diacetyl in rotting fruit attracts *C. elegans*
302 (Choi et al. 2016). The new assay allows worms to freely move on a large field and alter their
303 behavior towards the odor over time more similar to natural habitats.

304 Although tracking a single population over time has advantages, this results in each data
305 point being dependent on the previous data point. This leads to a decrease in resolution in data
306 over time that is not a problem in the standard assay. Due to this concern we tested whether
307 different behavioral states in *C. elegans* mutants can be resolved in the real-time assay. We
308 found that short-term odor memory defects were observed in *cng-3* mutants in the real-time
309 assay as has been observed in the standard assay (O'Halloran et al. 2017). Still, the standard
310 assay has stronger behavior resolving power than our new assay particularly in identifying
311 behavior mutants. The real-time assay cannot replace the standard behavior assay but can
312 supplement it with an ability to observe temporal dynamics on a large scale and also simulate
313 natural odor behaviors.

314 Using the real-time assay we were able to identify odors in which memory forms early in
315 *C. elegans* such as 1-methylpyrrole, and odors in which memory forms late such as 4-
316 chlorobenzyl mercaptan. Since formation of long-term memory to AWC-sensed odors requires
317 EGL-4 nuclear translocation, we exposed worms to early-trending and late-trending odors and
318 observed EGL-4 localization over time. We found a correlation between the timing of memory
319 formation and nuclear accumulation. How then do specific odors regulate the timing of EGL-4
320 nuclear translocation? Long-term odor memory in the AWC neuron is dependent on the
321 coincident detection of food deprivation that is mediated by insulin signaling from the AIA
322 neuron (Cho et al. 2016). Insulin signals from the AIA activate the PI3 kinase AGE-1 in the AWC
323 neuron to promote EGL-4 nuclear accumulation. However, food deprivation is stable from odor
324 to odor in our experiments, thus AIA neuron-dependent insulin signals likely cannot account for
325 the differences observed in odor-dependent EGL-4 nuclear translocation. Within the AWC
326 neuron, the G-protein ODR-3 and cGMP levels have both been shown to regulate nuclear EGL-4
327 localization (O'Halloran et al. 2009; O'Halloran et al. 2012). Specific odors, and possibly specific
328 G-protein coupled olfactory receptors, may target ODR-3 and/or cGMP machinery which
329 includes the guanylyl cyclases ODR-1 and DAF-11 and AWC-specific phosphodiesterases to
330 regulate the timing of EGL-4 nuclear localization (Birnby et al. 2000; L'Etoile & Bargmann 2000;
331 Roayaie et al. 1998). Further experiments that identify new olfactory receptors in the AWC
332 neuron will elucidate the specific mechanisms.

333 One possible explanation of the differences in odor memory formation is that odor
334 attraction and memory is concentration-dependent. For this reason, we tested several dilutions
335 for most of the odors analyzed in the real-time behavior assay (data not shown), and finally

336 chose the optimal dilution for each odor in which behavior change was greatest over the entire
337 experiment. In this way, we observed that the collective change in attraction over the whole
338 assay was very similar for 12 of 13 odors tested. Despite overall similarities at the optimal
339 concentrations, temporal patterns of behavior change were still varied among the odors.

340 We also tested memory formation to the AWA-sensed odor diacetyl and found that
341 memory formed faster and more consistently than AWC-sensed odors. In addition, the odor
342 2,4,5-trimethylthiazole is sensed by both AWA and AWC neurons. Interestingly, we found that
343 2,4,5-TMT induced EGL-4 nuclear accumulation in the AWC neuron, and memory formation was
344 correlated to late EGL-4 translocation. Further testing with AWA-sensed odors such as pyrazine
345 (Bargmann et al. 1993) and butyric acid and isobutyric acid (Table 1) may reveal whether
346 fundamentally different mechanisms of odor memory formation exist between the AWA and
347 AWC neurons.

348 In this study, we investigated *C. elegans* response to many odors, including odors that
349 have not been tested on *C. elegans* before, and identified the sensory neuron responsible for
350 each odor attraction. In addition, we tested the memory formation towards 13 of the odors
351 over time. Such inherent behaviors towards the odors indicates that these odors may be
352 ecologically relevant cues for *C. elegans* in nature. For instance, 2-isobutylthiazole is a major
353 component of antelope pheromone (Burger et al. 1988), 2-methylpyrazine is the main volatile
354 component of grape vinegar (Pinu et al. 2016), and butyric acid is produced by microbial
355 fermentation (Pasteur 1861). Indeed, studies have shown ecologically relevant relationships
356 between *C. elegans* and diacetyl (Choi et al. 2016), methyl 3-methyl-2-butenoate (Hsueh et al.
357 2017), and 2-heptanone (Zhang et al. 2016), and mammalian predator-prey relationships

358 between 2,4,5-TMT, a component of fox feces, and rodents (Vernet-Maury 1980). Finally, we
359 found that memory does not form towards cyclohexylethanol. The ecological implications of a
360 persistent attraction to this odor is unknown. Cyclohexylethanol derivatives were found in a
361 plant root extract widely used in Chinese folk medicine (Huang et al. 2009), but relationships
362 with nematodes need to be further investigated. We hope that this study can be a platform for
363 more studies into natural odor behaviors.

364

365 **CONCLUSION**

366 Dynamics of memory formation may vary depending on the cue that is learned. Since *C.*
367 *elegans* can form memories to a multitude of odor cues, we devised a new behavioral assay to
368 efficiently examine the temporal dynamics of odor memory formation to over a dozen odors.
369 Using the real-time behavior assay, we found that worms form memories to certain odors
370 faster than others. Finally, we investigated the cellular basis for this difference and found that
371 rate of EGL-4 nuclear translocation for each odor was correlated to the rate of memory
372 formation.

373

374 **ACKNOWLEDGEMENTS**

375 We would like to thank the Caenorhabditis Genetic Center which is supported by the by NIH
376 Office of Research Infrastructure Programs for strains, and the Korean Creative Foundation for
377 the Undergraduate Research Program.

378

379 **FIGURE LEGENDS**

380 Figure 1. Real-time odor behavior assay. (A) Assay design. Worms are placed in the middle of a
381 15 cm square plate. Odor solution is placed on one side of the plate, and a weak
382 counterattractant (*E. coli* strain OP50) is placed on the opposite side. (B) Benzaldehyde
383 attraction in real-time odor behavior assay. Attraction to the odor benzaldehyde (blue)
384 decreases over the 2 hour assay. Control diluent (100% ethanol) attraction is shown in red.

385

386 Figure 2. Short-term and long-term odor memory to the odor benzaldehyde in the real-time
387 odor behavior assay. Attraction over time with N2 wild type, *cng-3* short-term odor memory
388 defective mutants, and *adp-1* short-term and long-term odor memory mutants in the standard
389 behavior assay (A) and the real-time odor behavior assay (B). (C) Short-term odor memory in
390 the standard and real-time behavior assays. Comparison of the 0' and 40' minute time points in
391 (A) with the 30' and 70' minute time points in (B) for N2 and *cng-3* mutants. Error bars indicate
392 standard error. Statistical significance calculated by student's T-test. * indicates $p<0.05$, **
393 indicates $p<0.001$, NS indicates not significant.

394

395 Figure 3. Temporal dynamics of odor memory to 12 odors. Purple dotted line marks
396 approximate place where 50% of total behavior change occurs for each odor. Error bars
397 indicate standard error.

398

399 Figure 4. GFP::EGL-4 nuclear accumulation in early and late trending odors. Animals were
400 exposed to odor for indicated time and cytoplasmic/nuclear GFP::EGL-4 localization was
401 observed. Early-trending odors are on the left, and late-trending odors on the right. A
402 polynomial regression was calculated and regression curves are indicated on each graph. See
403 Methods for individual regression equations. Error bars indicate standard error.

404

405 Table 1. AWC and AWA primary sensory neurons primary sensory neurons mediate the
406 attraction to 17 odors. Wild-type indicates N2 strain, AWC- indicates the ceh-36 mutant strain,
407 AWA- indicates odr-7 mutant strain. Right column indicates the neuron(s) responsible for
408 sensing each odor. Extra large dot = 0.6-1.0 attraction index (AI), large dot = 0.4-0.6 AI, medium
409 dot = 0.2-0.4 AI, and small dot < 0.2 AI.

410

411 Table 2. Timing of behavior change correlates with timing of GFP::EGL-4 nuclear accumulation.
412 Minutes to 50% animals with nuclear EGL-4 was calculated from the polynomial regression
413 equation (see Methods) for each odor.

414

415 Figure S1. *adp-1* mutants do not display odor memory to 4-chlorobenzyl mercaptan and 2,4,5-
416 trimethylthiazole. Attraction to 4-chlorobenzyl mercaptan (top) and 2,4,5-trimethylthiazole

417 (bottom) in the real-time behavior assay in wild-type N2 (blue) and *adp-1* mutant animals
418 (orange). Error bars indicate standard error.

419

420 Figure S2. *C. elegans* displays late memory formation to 2,4,5-trimethylthiazole in the standard
421 assay. Wild-type N2 animals show early memory formation to the odor benzaldehyde (dark
422 blue), and late memory formation to 2,4,5-trimethylthiazole (red). Error bars indicate standard
423 error.

424

425 **REFERENCES**

426 Bacskai BJ, Hochner B, Mahaut-Smith M, Adams SR, Kaang BK, Kandel ER, and Tsien RY. 1993.
427 Spatially resolved dynamics of cAMP and protein kinase A subunits in Aplysia sensory
428 neurons. *Science* 260:222-226.
429 Bargmann CI, Hartwieg E, and Horvitz HR. 1993. Odorant-selective genes and neurons mediate
430 olfaction in C. elegans. *Cell* 74:515-527.
431 Birnby DA, Link EM, Vowels JJ, Tian H, Colacurcio PL, and Thomas JH. 2000. A transmembrane
432 guanylyl cyclase (DAF-11) and Hsp90 (DAF-21) regulate a common set of chemosensory
433 behaviors in caenorhabditis elegans. *Genetics* 155:85-104.
434 Brenner S. 1974. The genetics of Caenorhabditis elegans. *Genetics* 77:71-94.
435 Broad KD, Hinton MR, Keverne EB, and Kendrick KM. 2002. Involvement of the medial
436 prefrontal cortex in mediating behavioural responses to odour cues rather than
437 olfactory recognition memory. *Neuroscience* 114:715-729.

438 Burger BV, Pretorius PJ, Stander J, and Grierson GR. 1988. Mammalian pheromone studies, VII.
439 Identification of thiazole derivatives in the preorbital gland secretions of the grey duiker,
440 Sylvicapra grimmia, and the red duiker, Cephalophus natalensis. *Z Naturforsch C* 43:731-
441 736.
442 Castellucci V, Pinsker H, Kupfermann I, and Kandel ER. 1970. Neuronal mechanisms of
443 habituation and dishabituation of the gill-withdrawal reflex in Aplysia. *Science* 167:1745-
444 1748.
445 Castellucci VF, Blumenfeld H, Goelet P, and Kandel ER. 1989. Inhibitor of protein synthesis
446 blocks long-term behavioral sensitization in the isolated gill-withdrawal reflex of Aplysia.
447 *J Neurobiol* 20:1-9. 10.1002/neu.480200102
448 Cho CE, Brueggemann C, L'Etoile ND, and Bargmann CI. 2016. Parallel encoding of sensory
449 history and behavioral preference during Caenorhabditis elegans olfactory learning. *Elife*
450 5. 10.7554/eLife.14000
451 Choi JI, Yoon KH, Subbammal Kalichamy S, Yoon SS, and Il Lee J. 2016. A natural odor attraction
452 between lactic acid bacteria and the nematode Caenorhabditis elegans. *ISME J* 10:558-
453 567. 10.1038/ismej.2015.134
454 Colbert HA, and Bargmann CI. 1995. Odorant-specific adaptation pathways generate olfactory
455 plasticity in C. elegans. *Neuron* 14:803-812.
456 Ghirardi M, Montarolo PG, and Kandel ER. 1995. A novel intermediate stage in the transition
457 between short- and long-term facilitation in the sensory to motor neuron synapse of
458 aplysia. *Neuron* 14:413-420.

459 Hawkins RD, Kandel ER, and Bailey CH. 2006. Molecular mechanisms of memory storage in
460 Aplysia. *Biol Bull* 210:174-191. 10.2307/4134556
461 Hsueh YP, Gronquist MR, Schwarz EM, Nath RD, Lee CH, Gharib S, Schroeder FC, and Sternberg
462 PW. 2017. Nematophagous fungus Arthrobotrys oligospora mimics olfactory cues of sex
463 and food to lure its nematode prey. *Elife* 6. 10.7554/eLife.20023
464 Huang ZS, Pei YH, Shen YH, Lin S, Liu CM, Lu M, and Zhang WD. 2009. Cyclohexyl-ethanol
465 derivatives from the roots of Incarvillea mairei. *J Asian Nat Prod Res* 11:523-528.
466 10.1080/10286020902927872
467 Juang BT, Gu C, Starnes L, Palladino F, Goga A, Kennedy S, and L'Etoile ND. 2013. Endogenous
468 nuclear RNAi mediates behavioral adaptation to odor. *Cell* 154:1010-1022.
469 10.1016/j.cell.2013.08.006
470 Kauffman AL, Ashraf JM, Corces-Zimmerman MR, Landis JN, and Murphy CT. 2010. Insulin
471 signaling and dietary restriction differentially influence the decline of learning and
472 memory with age. *PLoS Biol* 8:e1000372. 10.1371/journal.pbio.1000372
473 Klein M, Camardo J, and Kandel ER. 1982. Serotonin modulates a specific potassium current in
474 the sensory neurons that show presynaptic facilitation in Aplysia. *Proc Natl Acad Sci U S*
475 *A* 79:5713-5717.
476 L'Etoile ND, and Bargmann CI. 2000. Olfaction and odor discrimination are mediated by the C.
477 elegans guanylyl cyclase ODR-1. *Neuron* 25:575-586.
478 L'Etoile ND, Coburn CM, Eastham J, Kistler A, Gallegos G, and Bargmann CI. 2002. The cyclic
479 GMP-dependent protein kinase EGL-4 regulates olfactory adaptation in C. elegans.
480 *Neuron* 36:1079-1089.

481 Lanjuin A, VanHoven MK, Bargmann CI, Thompson JK, and Sengupta P. 2003. Otx/otd
482 homeobox genes specify distinct sensory neuron identities in C. elegans. *Dev Cell* 5:621-
483 633.
484 Lee JI, O'Halloran DM, Eastham-Anderson J, Juang BT, Kaye JA, Scott Hamilton O, Lesch B, Goga
485 A, and L'Etoile ND. 2010. Nuclear entry of a cGMP-dependent kinase converts transient
486 into long-lasting olfactory adaptation. *Proc Natl Acad Sci U S A* 107:6016-6021.
487 10.1073/pnas.1000866107
488 Levy F, Keller M, and Poindron P. 2004. Olfactory regulation of maternal behavior in mammals.
489 *Horm Behav* 46:284-302. 10.1016/j.yhbeh.2004.02.005
490 Lin CH, Tomioka M, Pereira S, Sellings L, Iino Y, and van der Kooy D. 2010. Insulin signaling plays
491 a dual role in Caenorhabditis elegans memory acquisition and memory retrieval. *J*
492 *Neurosci* 30:8001-8011. 10.1523/JNEUROSCI.4636-09.2010
493 Mansuy IM, Mayford M, Jacob B, Kandel ER, and Bach ME. 1998. Restricted and regulated
494 overexpression reveals calcineurin as a key component in the transition from short-term
495 to long-term memory. *Cell* 92:39-49.
496 Montarolo PG, Goelet P, Castellucci VF, Morgan J, Kandel ER, and Schacher S. 1986. A critical
497 period for macromolecular synthesis in long-term heterosynaptic facilitation in Aplysia.
498 *Science* 234:1249-1254.
499 O'Halloran DM, Altshuler-Keylin S, Lee JI, and L'Etoile ND. 2009. Regulators of AWC-mediated
500 olfactory plasticity in Caenorhabditis elegans. *PLoS Genet* 5:e1000761.
501 10.1371/journal.pgen.1000761

502 O'Halloran DM, Altshuler-Keylin S, Zhang XD, He C, Morales-Phan C, Yu Y, Kaye JA,
503 Brueggemann C, Chen TY, and L'Etoile ND. 2017. Contribution of the cyclic nucleotide
504 gated channel subunit, CNG-3, to olfactory plasticity in Caenorhabditis elegans. *Sci Rep*
505 7:169. 10.1038/s41598-017-00126-7
506 O'Halloran DM, Hamilton OS, Lee JI, Gallegos M, and L'Etoile ND. 2012. Changes in cGMP levels
507 affect the localization of EGL-4 in AWC in Caenorhabditis elegans. *PLoS One* 7:e31614.
508 10.1371/journal.pone.0031614
509 Pasteur L. 1861. On the viscous fermentation and the butyrous fermentation. *Bulletin de la*
510 *Société Chimique de France* 11:30–31.
511 Pinu FR, de Carvalho-Silva S, Trovatti Uetanabaro AP, and Villas-Boas SG. 2016. Vinegar
512 Metabolomics: An Explorative Study of Commercial Balsamic Vinegars Using Gas
513 Chromatography-Mass Spectrometry. *Metabolites* 6. 10.3390/metabo6030022
514 Purcell AL, Sharma SK, Bagnall MW, Sutton MA, and Carew TJ. 2003. Activation of a tyrosine
515 kinase-MAPK cascade enhances the induction of long-term synaptic facilitation and
516 long-term memory in Aplysia. *Neuron* 37:473-484.
517 Remy JJ, and Hobert O. 2005. An interneuronal chemoreceptor required for olfactory imprinting
518 in C. elegans. *Science* 309:787-790. 10.1126/science.1114209
519 Roayaie K, Crump JG, Sagasti A, and Bargmann CI. 1998. The G alpha protein ODR-3 mediates
520 olfactory and nociceptive function and controls cilium morphogenesis in C. elegans
521 olfactory neurons. *Neuron* 20:55-67.
522 Sengupta P, Colbert HA, and Bargmann CI. 1994. The C. elegans gene odr-7 encodes an
523 olfactory-specific member of the nuclear receptor superfamily. *Cell* 79:971-980.

524 Sutton MA, Masters SE, Bagnall MW, and Carew TJ. 2001. Molecular mechanisms underlying a
525 unique intermediate phase of memory in aplysia. *Neuron* 31:143-154.
526 Torayama I, Ishihara T, and Katsura I. 2007. Caenorhabditis elegans integrates the signals of
527 butanone and food to enhance chemotaxis to butanone. *J Neurosci* 27:741-750.
528 10.1523/JNEUROSCI.4312-06.2007
529 Vernet-Maury E. 1980. Trimethyl-thiazoline in fox feces: A natural alarming substance for the
530 rat In: Van Der Starr H, editor. International Symposium on Olfaction and Taste: IRL
531 Press. p 407.
532 Ward S. 1973. Chemotaxis by the nematode Caenorhabditis elegans: identification of
533 attractants and analysis of the response by use of mutants. *Proc Natl Acad Sci U S A*
534 70:817-821.
535 Zhang C, Zhao N, Chen Y, Zhang D, Yan J, Zou W, Zhang K, and Huang X. 2016. The Signaling
536 Pathway of Caenorhabditis elegans Mediates Chemotaxis Response to the Attractant 2-
537 Heptanone in a Trojan Horse-like Pathogenesis. *J Biol Chem* 291:23618-23627.
538 10.1074/jbc.M116.741132

539

Table 1(on next page)

AWC and AWA primary sensory neurons primary sensory neurons mediate the attraction to 17 odors.

Wild-type indicates N2 strain, AWC- indicates the ceh-36 mutant strain, AWA- indicates odr-7 mutant strain. Right column indicates the neuron(s) responsible for sensing each odor. Extra large dot = 0.6-1.0 attraction index (AI), large dot = 0.4-0.6 AI, medium dot = 0.2-0.4 AI, and small dot < 0.2 AI.

PeerJ Preprints NOT PEER-REVIEWED

odor	wild-type	AWC-	AWA-	AWA/AWC
diacetyl	●	●	•	AWA
benzaldehyde	●	•	●	AWC
butanone	●	•	●	AWC
isobutyric acid	●	●	•	AWA
2-isobutyl thiazole	●	●	●	AWC
dimethylthiazole	●	●	●	AWC
2,4,5-trimethylthiazole	●	●	●	AWA or AWC
2-methylpyrazine	●	•	●	AWC
2-heptanone	●	•	●	AWC
1-methylpyrrole	●	•	●	AWC
4-chlorobenzyl mercaptan	●	•	●	AWC
butyric acid	●	●	•	AWA
1-pentanol	●	•	●	AWC
benzyl mercaptan	●	•	●	AWC
2-cyclohexylethanol	●	•	●	AWC
2-ethoxythiazole	●	•	●	AWC
benzyl proprionate	●	●	•	AWA and AWC

PeerJ Preprints | https://doi.org/10.7287/peerj.preprints.26451v1 | CC BY 4.0 Open Access | rec: 22 Jan 2018, publ: 22 Jan 2018

Table 2 (on next page)

Timing of behavior change correlates with timing of GFP::EGL-4 nuclear accumulation.

Minutes to 50% animals with nuclear EGL-4 was calculated from the polynomial regression equation (see Methods) for each odor.

PeerJ Preprints NOT PEER-REVIEWED

odor	Minutes to 50% behavior change	Minutes to 50% animals with nuclear EGL-4
1-methylpyrrole	80	76.6
2-ethoxythiazole	90	59.2
benzaldehyde	90	69.7
4-chlorobenzyl mercaptan	100	88.44
2,4,5-trimethylthiazole	110	90.96

PeerJ Preprints | https://doi.org/10.7287/peerj.preprints.26451v1 | CC BY 4.0 Open Access | rec: 22 Jan 2018, publ: 22 Jan 2018

Figure 1(on next page)

Real-time odor behavior assay.

(A) Assay design. Worms are placed in the middle of a 15 cm square plate. Odor solution is placed on one side of the plate, and a weak counterattractant (*E. coli* strain OP50) is placed on the opposite side. (B) Benzaldehyde attraction in real-time odor behavior assay. Attraction to the odor benzaldehyde (blue) decreases over the 2 hour assay. Control diluent (100% ethanol) attraction is shown in red.

PeerJ Preprints NOT PEER-REVIEWED

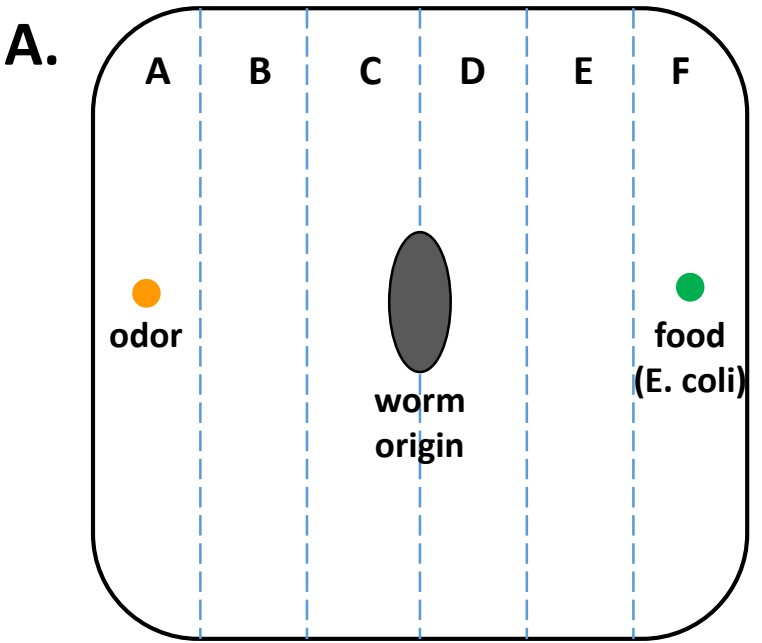

$$\text{Attraction index} = \frac{(2A + B) - (E + 2F)}{2(A+B+E+F)}$$

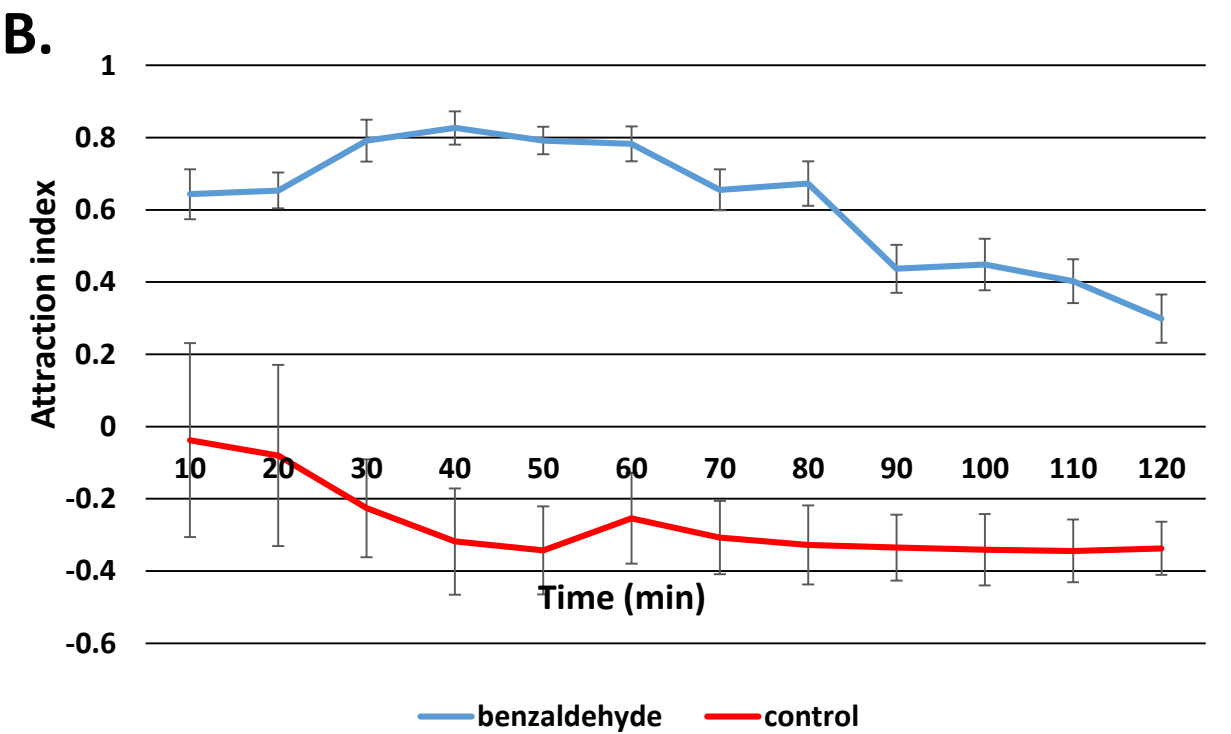

PeerJ Preprints | https://doi.org/10.7287/peerj.preprints.26451v1 | CC BY 4.0 Open Access | rec: 22 Jan 2018, publ: 22 Jan 2018

Figure 2(on next page)

Short-term and long-term odor memory to the odor benzaldehyde in the real-time odor behavior assay.

Attraction over time with N2 wild type, *cng-3* short-term odor memory defective mutants, and *adp-1* short-term and long-term odor memory mutants in the standard behavior assay (A) and the real-time odor behavior assay (B). (C) Short-term odor memory in the standard and real-time behavior assays. Comparison of the 0’ and 40’ minute time points in (A) with the 30’ and 70’ minute time points in (B) for N2 and *cng-3* mutants. Error bars indicate standard error. Statistical significance calculated by student’s T-test. * indicates $p<0.05$, ** indicates $p<0.001$, NS indicates not significant.

PeerJ Preprints NOT PEER-REVIEWED

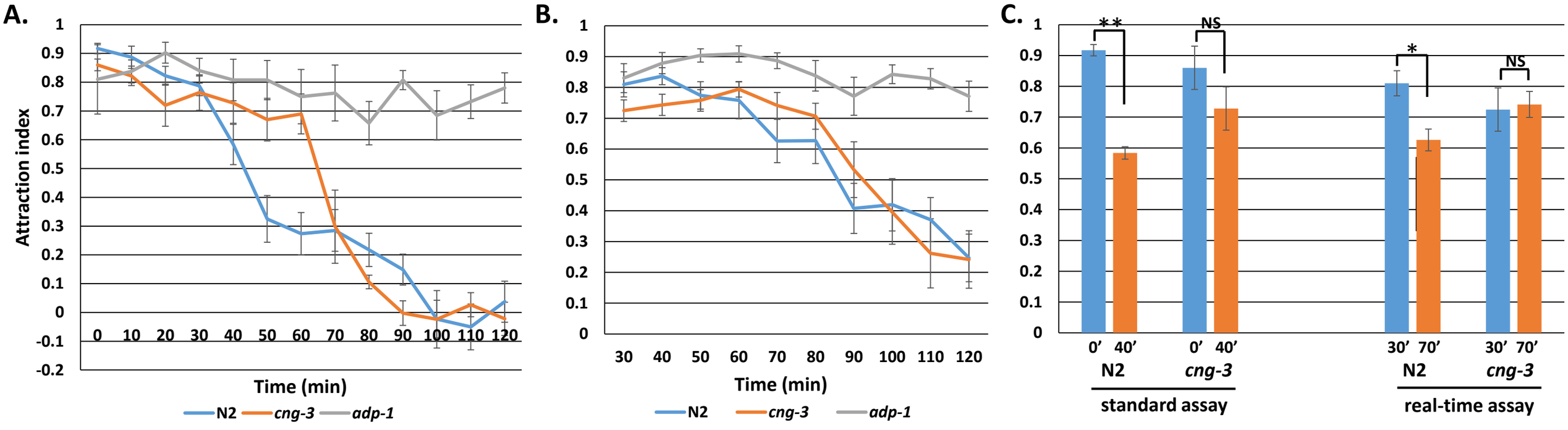

Peerj Preprints | https://doi.org/10.7287/peerj.preprints.26451v1 | CC BY 4.0 Open Access | rec: 22 Jan 2018, publ: 22 Jan 2018

Figure 3(on next page)

Temporal dynamics of odor memory for 12 different odors.

Purple dotted line marks approximate place where 50% of total behavior change occurs for each odor. Error bars indicate standard error.

PeerJ Preprints NOT PEER-REVIEWED

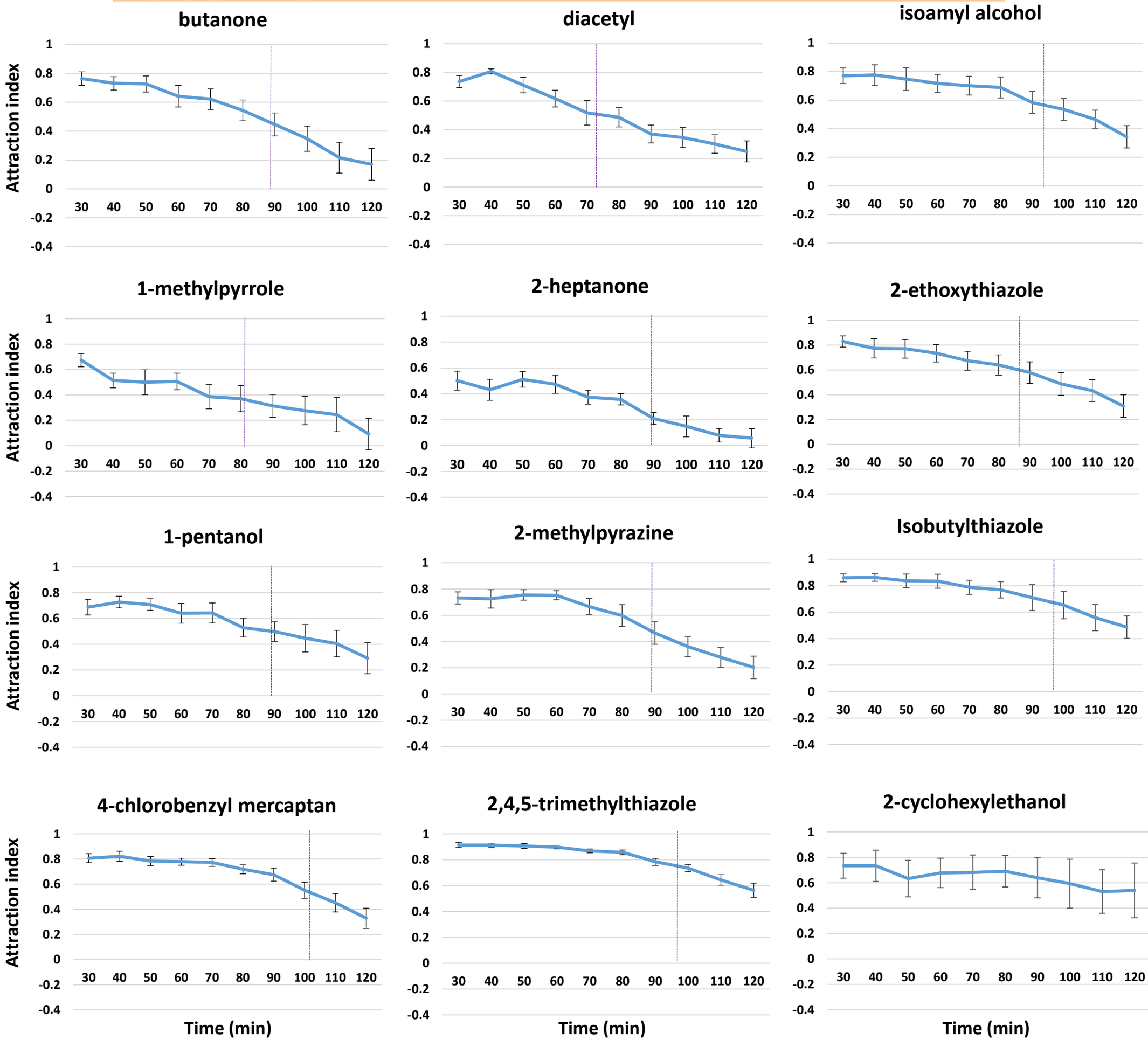

PeerJ Preprints | https://doi.org/10.7287/peerj.preprints.26451v1 | CC BY 4.0 Open Access | rec: 22 Jan 2018, publ: 22 Jan 2018

Figure 4(on next page)

GFP::EGL-4 nuclear accumulation in early and late trending odors.

Animals were exposed to odor for indicated time and cytoplasmic/nuclear GFP::EGL-4 localization was observed. Early-trending odors are on the left, and late-trending odors on the right. A polynomial regression was calculated and regression curves are indicated on each graph. See Methods for individual regression equations. Error bars indicate standard error.

PeerJ Preprints NOT PEER-REVIEWED

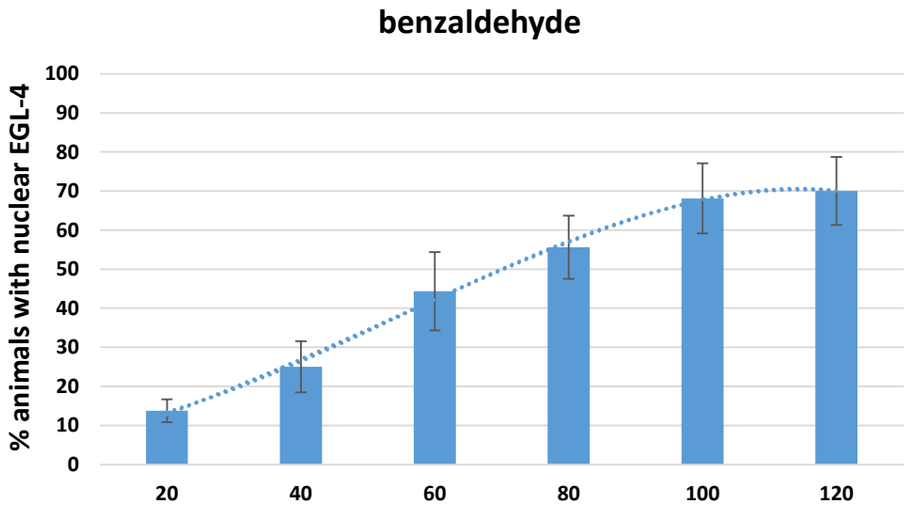

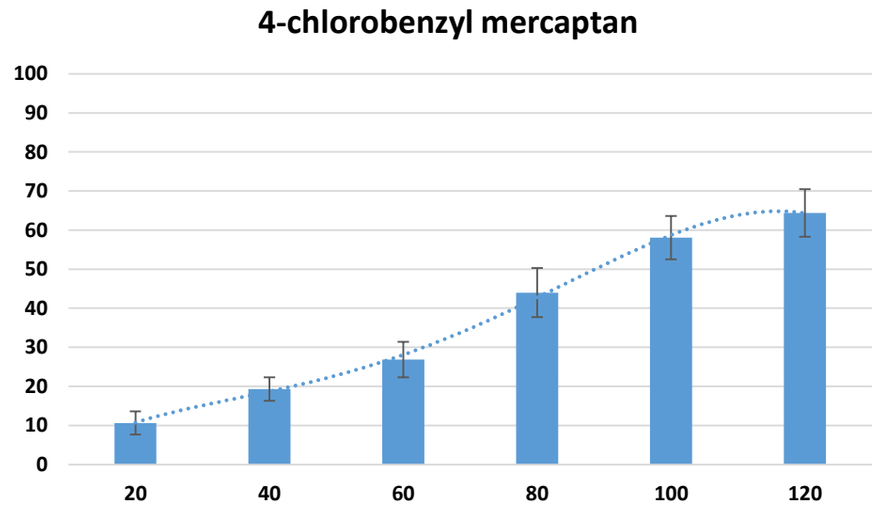

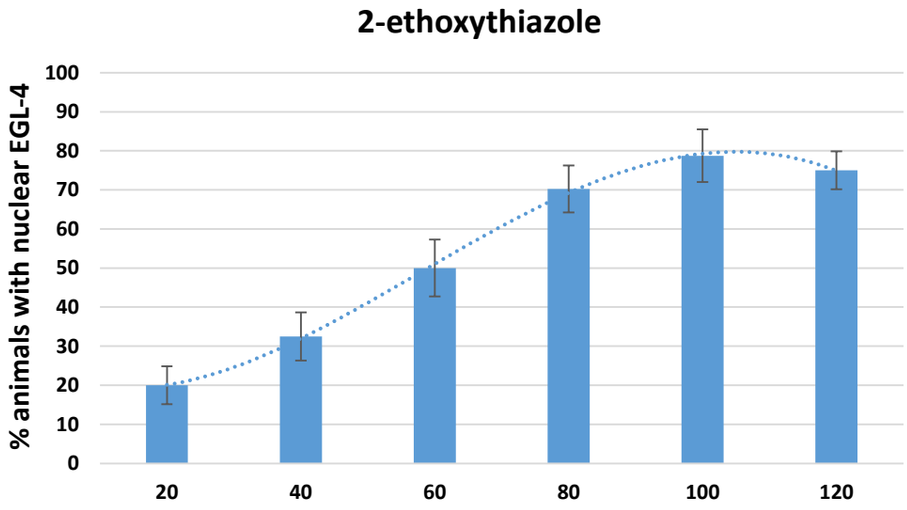

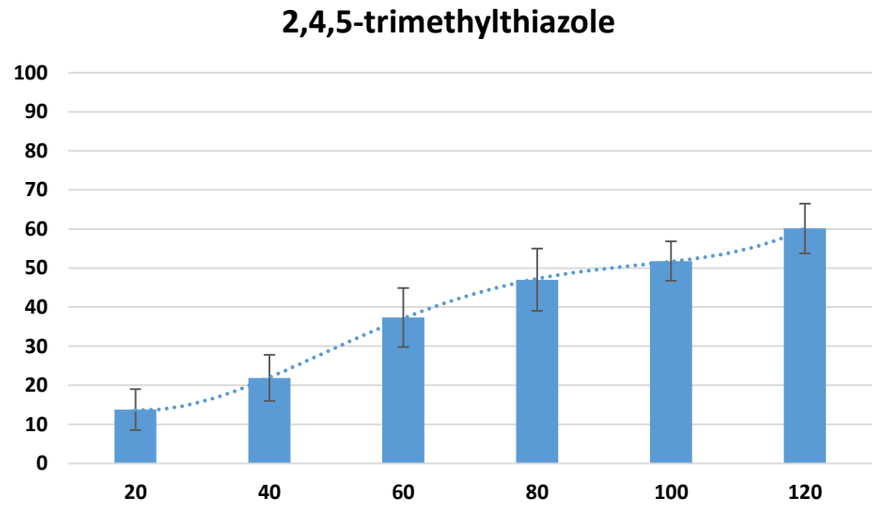

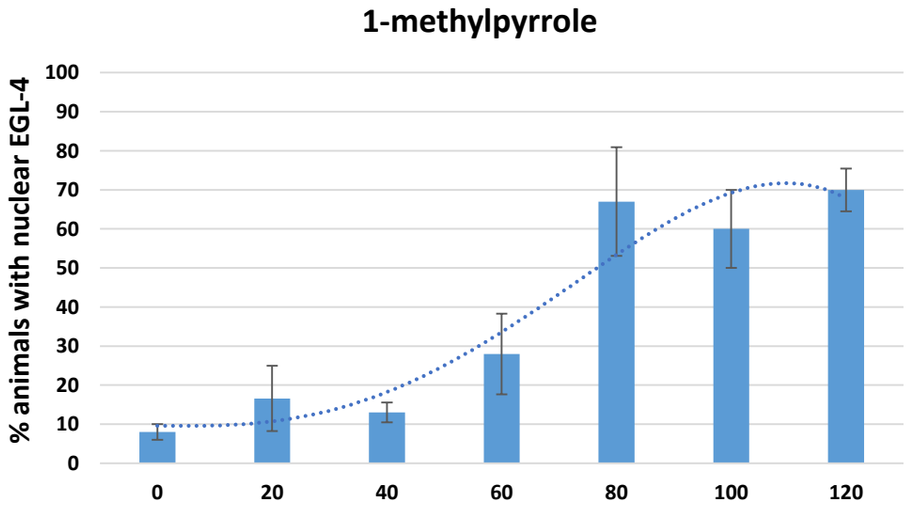

PeerJ Preprints | https://doi.org/10.7287/peerj.preprints.26451v1 | CC BY 4.0 Open Access | rec: 22 Jan 2018, publ: 22 Jan 2018